OBSERVATION OF DAYTIME CHANGES
IN BOUNDARY LAYER
ON A CLEAR AND WEAK-WIND SUMMER DAY
IN WESTERN SUBURBAN OF TOKYO

**Masato I. NODZU, Jun MATSUMOTO, Takanori WATANABE,
Yoshihito SETO, Ko NAKAJIMA*, Tomoshige INOUE****
and Jun-Ichi HAMADA

Abstract   Temperature, relative humidity, and wind conditions were observed on a clear, hot, summer day on 6 August 2019, 07:30–15:30 local time (LT), near the surface and in the boundary layer at the Minami-Osawa Campus of Tokyo Metropolitan University in the western suburb of Tokyo, Japan. Vertical wind profiles were obtained by pilot-balloon observations (PBOs) and unmanned aerial vehicle (UAV) observations. PBOs and surface wind observations revealed a southerly wind in the lower boundary layer from 11:00 LT, which became stronger during 12:30–15:30 LT. Temperature plateaued at 11:00–13:00 LT near the surface, whereas a sharp peak was observed by the UAV in the surface boundary layer at 11:00 LT. Water-vapor mixing ratios were higher in the afternoon than in the morning, with heavy cloud cover after 14:30 LT. Comparison with PBO data indicated that wind-speed estimations based on UAV flight-attitude information are problematic.

Keywords: summer heat, diurnal change, atmospheric boundary layer, vertical profile, unmanned aerial vehicle

1. Introduction

High-resolution vertical observations are necessary for understanding of the atmospheric boundary layer (ABL) due to its significant diurnal variation. Although in situ vertical observations with high spatio-temporal resolution were difficult, especially in urban areas (e.g., Shea and Auer 1978), they have been attempted at conducting with unmanned aerial vehicles (UAVs) in recent years (Elston *et al.* 2015). For example, diurnal changes were observed with UAV-borne instruments in nocturnal surface inversion (Flores *et al.* 2020) or urban areas (e.g., Sekula *et al.* 2021). It has been found that UAV observations are within 0.8°C and 8% of radiosonde observations of temperature and relative humidity (RH), respectively (Koch *et al.* 2018). Moreover, some studies

*Fukushima Renewable Energy Institute, AIST (FREA), National Institute of Advanced Industrial Science and Technology (AIST), Japan
**Faculty of Life and Environmental Sciences, University of Tsukuba, Japan

demonstrated improvement in numerical weather forecasts by assimilating high-resolution data from UAV observations which could not be obtained from conventional observations (Leuenberger *et al.* 2020).

One challenging issue is measuring winds with UAVs. Wind observations by UAVs often use hypersonic anemometers in the ABL (e.g., Shimura *et al.* 2018). Wind estimation from attitude information of a UAV was verified near the ground (e.g., Palomaki *et al.* 2017), whereas that in the ABL has not been sufficiently verified.

Here we report observations of vertical wind profiles ("wind" hereinafter refers to wind speed and direction) using pilot balloons and trials of UAVs in obtaining vertical profiles of temperature, RH, and wind to clarify temporal changes in surface boundary layer conditions on 6 August 2019, which was a weak-wind, clear summer day in Tokyo, Japan.

2. Observations, data, and methods

Observations

The observations were conducted at the Minami-Osawa Campus of Tokyo Metropolitan University (35°37′N, 139°23′E), in a residential area of Hachioji, 35 km west of central Tokyo in the Kanto region (Fig. 1). The observation site is a grassland with a single hill of radius ~40 m surrounded by flat land beside forest on its eastern and southern sides, some trees on the northern and southwestern sides, and a main campus road on the western side.
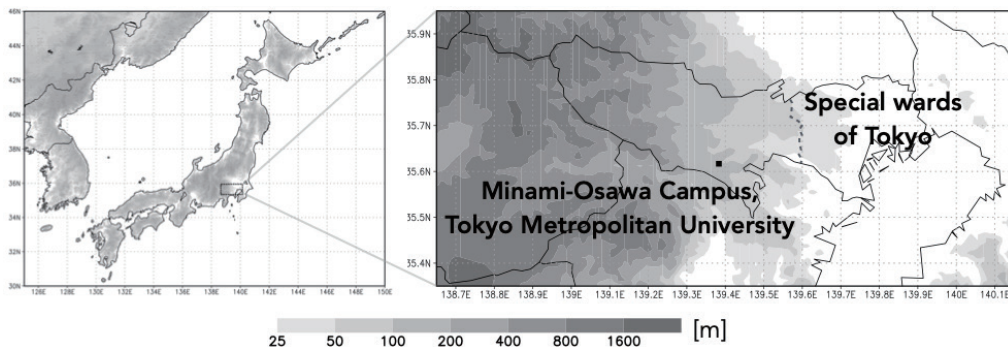

Fig. 1   Topography (gray shading) over (left) the main part of Japan and (right) near the Minami-Osawa Campus and Tokyo. The western border of the Special wards of Tokyo is drawn with the dashed curve. Topographic data were taken from Global Land One-km Base Elevation (GLOBE) data, distributed by the GLOBE Project (Hastings and Dunbar 1999).

Pilot balloons and a UAV-borne instrument (model WP 2050 UL; Weather Information & Communications Services Ltd., Tokyo, Japan) were used to obtain vertical profiles of wind, temperature, RH, and atmospheric pressure. Pilot-balloon observations (PBOs) and UAV flights were conducted at intervals of approximately 30 min during 07:30–15:30 and 07:32–15:02 local time (LT), respectively. Times varied slightly owing to operational and safety requirements, but intervals of nominally 30 min were assumed in the analysis. Balloons were launched from the hilltop

and observed using a theodolite (TD-4; Tamaya Technics Inc., Tokyo, Japan) installed on the adjacent flat land. The UAV (Matrice model M210 RTK; SZ DJI Technology Co., Ltd., Shenzhen, China) was launched from the flat land and flew vertically with no horizontal movement.

PBOs involved adjustment of the ascent speed to 2.5 m s^{-1} by filling with helium to a buoyancy of 56 g. Balloon azimuth and elevation were recorded at 2 s intervals over a flight time of typically 15 min, during which a vertical wind profile was recorded to an altitude of up to 2.25 km.

The UAV flights started 1–2 min after each balloon launch, with sensors mounted on UAV legs. Downwash was evident within 10 m of the UAV, so data obtained during descent were mainly used. Considering of the sensors' time constant, data obtained in the hovering period were analyzed in detail.

An Assmann's aspiration psychrometer was installed under trees facing the main road northwest of the site to observe surface temperature and RH. A portable micro-anemometer was installed on the hilltop. Cloud amounts (CAs) of 0–10 were observed visually.

On 6 August 2019, the site was covered by the subtropical Pacific High extending from the east. A small typhoon in the Kyushu district moved northwestward but did not affect the meteorological status of the site. In the morning, infrared images from the Himawari 8 geostationary weather satellite indicated that the Kanto district was not covered by cloud; however, cloud systems were generated in the northern mountainous Kanto regions from about 13:00 LT, and some upper-level clouds reached the site.

Methods

Vertical PBO wind profiles were based on an assumed ascent rate of 2.5 m s^{-1}, and UAV heights were estimated from continuous temperature, RH, and pressure data assuming hydrostatic equilibrium. Temperature and RH were defined as mean values for each independent continuous UAV hovering period with pressure changes of < 0.5 hPa in the preceding 30 s. UAV wind data were compiled using a wind estimation service provided by Airdata UAV (2015), based on UAV attitude data.

3. Results

Surface observations

Firstly, we show time series of the surface observations. Before 09:30 LT, temperature and RH were variable (Fig. 2a), with CA < 4 and southeasterly winds of < 1.0 m s^{-1} (Fig. 2b). During 10:00–11:00 LT, there was a rapid increase in temperature and a decrease in RH. CA peaked at 10:00 LT, and southeasterly wind continued at 0.6–0.9 m s^{-1}. Temperature plateaued at 11:00–13:00 LT with low CA, increased wind speed and RH. Temperature decreased after 13:00 LT, and RH decreased during 13:30–14:00 LT. The CA increased to 9 at 15:30. Wind speed was maintained at > 1.5 m s^{-1}, and the wind direction was easterly and southerly before and after 14:30 LT, respectively.

Next, we describe vertical profiles of wind from the PBO. Most pilot balloons reached altitudes of 2.2 km with multi-layer observations of wind speeds exceeding 2.0 m s^{-1} (Fig. 3). Observations were considered as the early, transitional, and late periods; 07:30–10:00, 10:30–11:30, and 12:30–15:30 LT, respectively. During the early period, triple layers with wind speeds exceeding 2.0 m s^{-1} were observed at approximately 2.0 and 1.3 km heights and near the ground level. Southerly winds
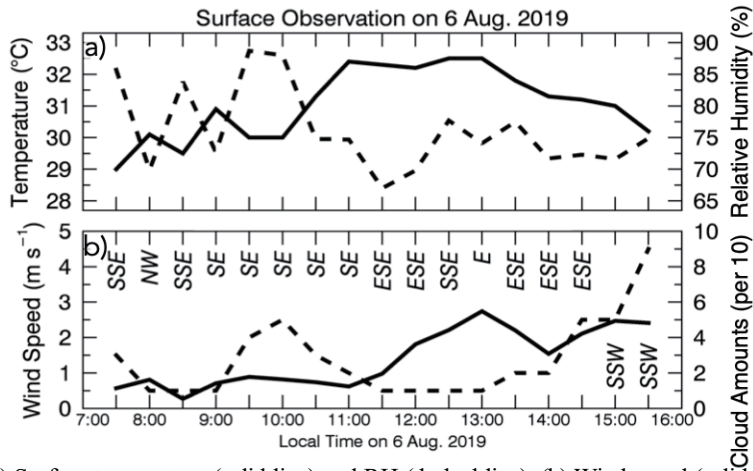
Fig. 2 (a) Surface temperature (solid line) and RH (dashed line). (b) Wind speed (solid line), cloud amount (dashed line), and wind direction (italic texts) on 6 Aug. 2019 at the observation site.
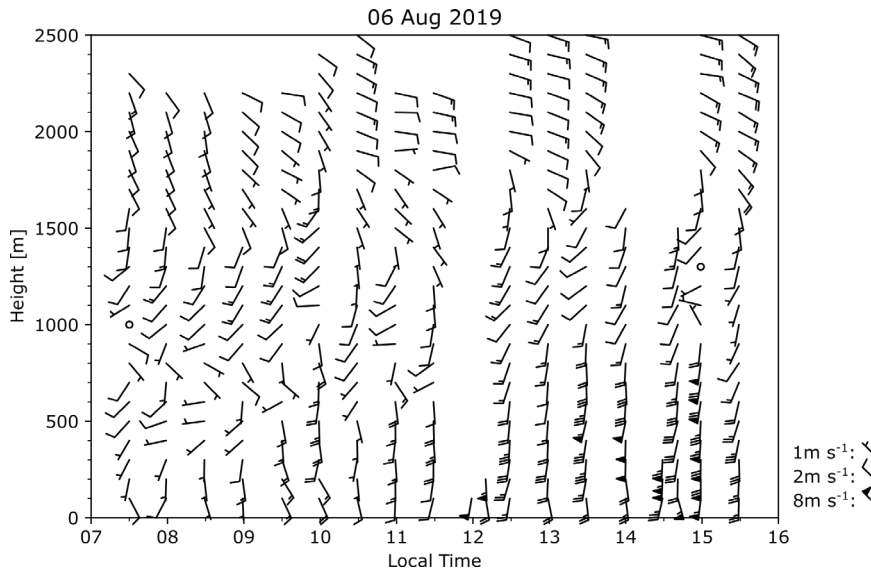

Fig. 3 Wind profiles shown by wind barbs at 100-m intervals observed by pilot balloons on 6 Aug. 2019 at the observation site.

were predominant in the upper and lower layers, whereas the middle layer had westerly components of > 1.0 m s^{-1}. During the transitional period, the layer with wind speeds of < 2.0 m s^{-1}, between the middle and the lower layer with stronger winds, became unclear. In the lower (< 1.0 km) layer, the wind was southerly after 12:30 LT with speeds occasionally exceeding 8.0 m s^{-1}. Weaker southwesterly winds were observed at heights of 1.0–1.5 km. In the upper layer, easterly winds predominated after the transitional period, with speeds exceeding 3.0 m s^{-1}.

UAV observations of temperature and humidity

UAV observations by thermometer, hygrometer, and barometer are considered here as temperature and RH observations within the surface boundary layer. Profiles are shown in Fig. 4, which includes profiles obtained during the UAV ascent periods for reference. The following analysis was based on hovering periods during the descent.
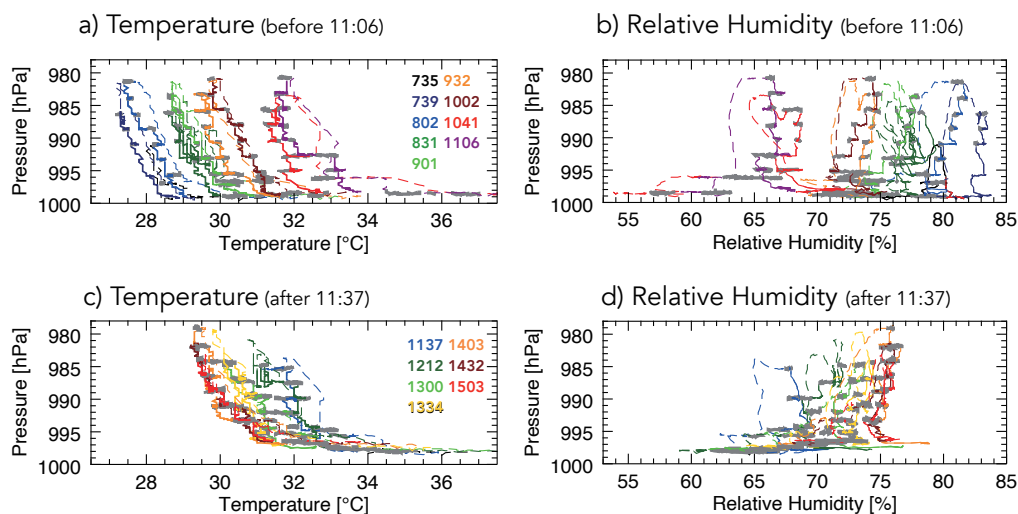

Fig. 4 (a, c) Temperature and (b, d) RH profiles observed by the UAV-borne thermometer, hygrometer, and barometer in the (a, b) first and (c, d) second halves of the observation period on 6 Aug. 2019. Solid and dashed lines indicate descent and ascent, respectively. Start times of UAV flights are indicated by the colors shown in (a, c). Hovering periods were defined by the time with a pressure change of < 0.5 hPa over the preceding 30 s, as shown by the thick gray lines.

Time series of vertical temperature and water-vapor mixing ratio profiles are shown in Fig. 5. Temperature displayed a temporal change with a peak at 11:00–12:00 LT (Fig. 5a). In surface observations, the temperature plateaued from 11:00 to 13:00 LT (Fig. 2a). The peak period of the lowest layer thus corresponded to the first half of the peak period of surface observation. The temperature in the layer below 15 m was sometimes higher than that at the surface (32–33 °C; Fig. 2a), and the high values of > 35 °C at 10:30 LT seemed to be associated with ground heating, possibly because of the difference in solar radiation exposure between UAV and surface observations. UAV-borne instruments may have recorded higher temperatures in sunshine than surface observations with sensors shaded by trees. Temperatures at heights of 15–150 m peaked at about 11:00 LT, contrasting with the plateau in surface and near-surface observations. Clear temporal changes were not evident in the vertical temperature gradient, which did not change significantly in the layer between 50 and 150 m.

The water-vapor mixing ratio increased during the morning, with no marked decrease in the afternoon (Fig. 5b). The ratio was clearly higher in the layer below 15 m. The difference in mixing ratio between heights of 15 and 150 m was < 1.0 g kg^{-1} before 09:00 LT and approximately 1.5 g kg^{-1} at 11:00 LT, higher than in the afternoon. The trend was consistent with variations in the
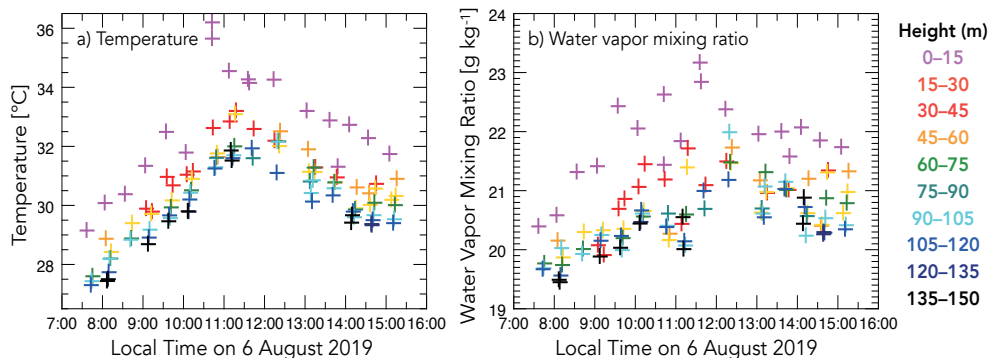
mixing ratio, independent of altitude.

Fig. 5 Time series in vertical profiles of (a) temperature and (b) water vapor mixing ratio with mean values for each hovering period on 6 Aug. 2019. Heights were estimated from profiles of pressure, temperature, and RH. 15 m vertical layers are categorized by color.

UAV and balloon wind observation comparison

Wind conditions estimated by the UAV (hereinafter "UAV wind") were compared with those of PBOs.

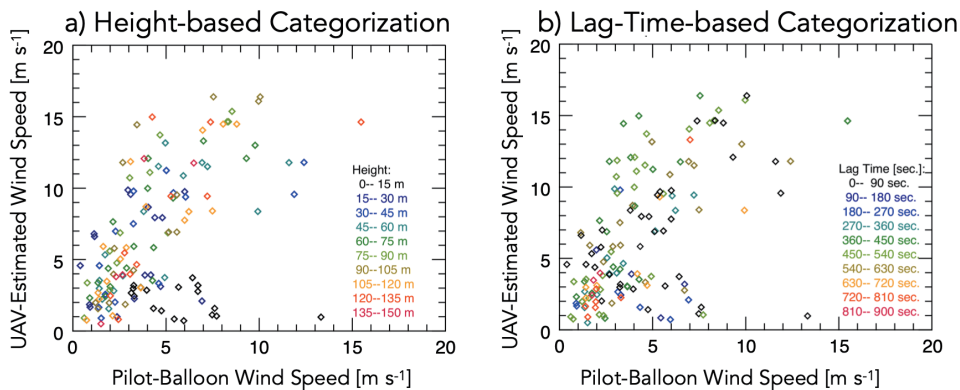Wind speeds from both observations are compared in Fig. 6. With PBO and UAV wind speeds

Fig. 6 Scatter diagrams comparing wind speeds between PBOs and UAV observations categorized by (a) height and (b) lag time.

of $< 4\ \mathrm{m\ s^{-1}}$, UAV values were distributed around PBO values. With PBO winds of $> 4\ \mathrm{m\ s^{-1}}$ and UAV wind of $< 4\ \mathrm{m\ s^{-1}}$, the underestimation of UAV wind relative to PBO values may be explained by large errors caused by the difficulty in observing the balloon using a theodolite near the surface with low observation heights (Fig. 6a). UAV wind speed was generally overestimated relative to PBO wind speed in cases with UAV wind speed of $> 4\ \mathrm{m\ s^{-1}}$. Time lag between the two

observations were not clearly related to lag time (Fig. 6b). This implies that the time lag did not greatly affect the comparison.

A wind-direction comparison (not shown) indicated insufficient sensitivity to direction, and further comparisons of PBOs and UAV observations are required.

4. Summary and Discussion

Wind profiles were observed using pilot balloons, and vertical profiles of temperature, humidity, and wind from a UAV were used to clarify temporal changes in the surface boundary layer on 6 August 2019 at a suburban site in western Tokyo. One of the most prominent features was the plateauing peak of temperature at 11:00–13:00 LT at the surface accompanied by cooling in the boundary layer. Assuming that cooling was brought by a southerly wind with a layer of around 500 m including the surface, it is necessary to consider that there was heating near the surface. Shortwave radiation is a candidate for heating near the surface by the persistent low CA between 11:00 and 13:00 LT.

After the temperature peak, the water-vapor mixing ratio remained higher than in the morning, whereas the CA increased until 15:30 LT. It is possible that the high humidity was maintained by local evapotranspiration. However, the satellite observation showed that the cloudiness expanded from the northern mountainous region (not shown). It is difficult to identify the source of water vapor whether from the local or the large region.

PBOs found weak and strong winds in the boundary layer in the morning and afternoon, respectively. The latter could be a southerly sea breeze, which might cause the plateaued surface temperature at 11:00–13:00 LT and a continuously high RH after 13:00 LT.

The potential sea breeze effect on the temporal change of wind in the ABL and the source of water vapor which maintained the high humidity after the temperature peak require further analysis of the horizontal distribution of temperature, humidity, and wind.

Temperature records have been found to vary with location of the sensor on a UAV (Inoue and Sato 2022), so errors must be continuously examined using UAV-borne instruments. The estimation of wind conditions based on flight attitude data may also include significant errors. Although such errors may be partly due to positional discrepancies between the UAV and balloons, they must be overcome for UAV use in aerological observations to be practicable in comparative pilot-balloon, radiosonde, and UAV-borne measurements.

References

Airdata UAV. 2015. Airdata UAV - Flight Data Analysis for Drones. https://app.airdata.com/ (November 30th, 2022).

Elston, J., Argrow, B., Stachura, M., Weibel, D., Lawrence, D. and Pope, D. 2015. Overview of small fixed-wing unmanned aircraft for meteorological sampling. *Journal of Atmospheric and Oceanic Technology* **32**: 97–115.

Flores, F., Arriagada, A., Donoso, N., Martínez, A., Viscarra, A., Falvey, M. and Schmitz, R. 2020. Investigation of a nocturnal cold-air pool in a semiclosed basin located in the Atacama Desert. *Journal of Applied Meteorology and Climatology* **59**: 1953–1970.

Hastings, D. A. and Dunbar, P. K. 1999. Global Land One-kilometer Base Elevation (GLOBE) digital elevation model, version 1.0. National Oceanic and Atmospheric Administration, National Geophysical Data Center, digital media. Available online at http://www.ngdc.noaa.gov/mgg/topo/globe.html (November 30th, 2022).

Inoue, J. and Sato, K. 2022. Toward sustainable meteorological profiling in polar regions: Case studies using an inexpensive UAS on measuring lower boundary layers with quality of radiosondes. *Environmental Research* **205**: 112468.

Koch, S. E., Fengler, M., Chilson, P. B., Elmore, K. L., Argrow, B., Andra, D. L. Jr. and Lindley, T. 2018. On the use of unmanned aircraft for sampling mesoscale phenomena in preconvective boundary layer. *Journal of Atmospheric and Oceanic Technology* **35**: 2265–2288.

Leuenberger, D., Haefele, A., Omanovic, N., Fengler, M., Martucci, G., Calpini, B., Fuhrer, O. and Rossa, A. 2020. Improving high-impact numerical weather prediction with lidar and drone observations. *Bulletin of the American Meteorological Society* **101**: E1036–E1051.

Palomaki, R. T., Rose, N. T., van den Bossche, M., Sherman, T. J. and De Wekker, S. F. 2017. Wind estimation in the lower atmosphere using multirotor aircraft. *Journal of Atmospheric and Oceanic Technology* **34**: 1183–1191.

Sekula, P., Zimnoch, M., Bartyzel, J., Bokwa, A., Kud, M. and Necki, J. 2021. Ultra-light airborne measurement system for investigation of urban boundary layer dynamics. *Sensors* **21**: 2920.

Shea, D. M. and Auer Jr., A. H. 1978. Thermodynamic properties and aerosol patterns in the plume downwind of St. Louis. *Journal of Applied Meteorology* **17**: 689–698.

Shimura, T., Inoue, M., Tsujimoto, H., Sasaki, K. and Iguchi, M. 2018. Estimation of wind vector profile using a hexarotor unmanned aerial vehicle and its application to Meteorological observation up to 1000 m above surface. *Journal of Atmospheric and Oceanic Technology* **35**: 1621–1631.